

## Self-adjuvanted L-arginine modified dextran-based nanogels for sustained local antigenic protein delivery to antigen presenting cells and enhanced cellular and humoral immune responses

Jin Teng Chung<sup>1</sup>, Mehrnoosh Rafiei<sup>1,2</sup>, Ying Chau<sup>1</sup>

<sup>1</sup>Department of Chemical and Biological Engineering, The Hong Kong University of Science and Technology, Hong Kong SAR, China

<sup>2</sup>Institute for Nanoscience and Nanotechnology, Sharif University of Technology, Tehran, Iran.

Keywords: nanoparticles; vaccine; immunotherapy; polysaccharides; amino acids

### Supplementary information

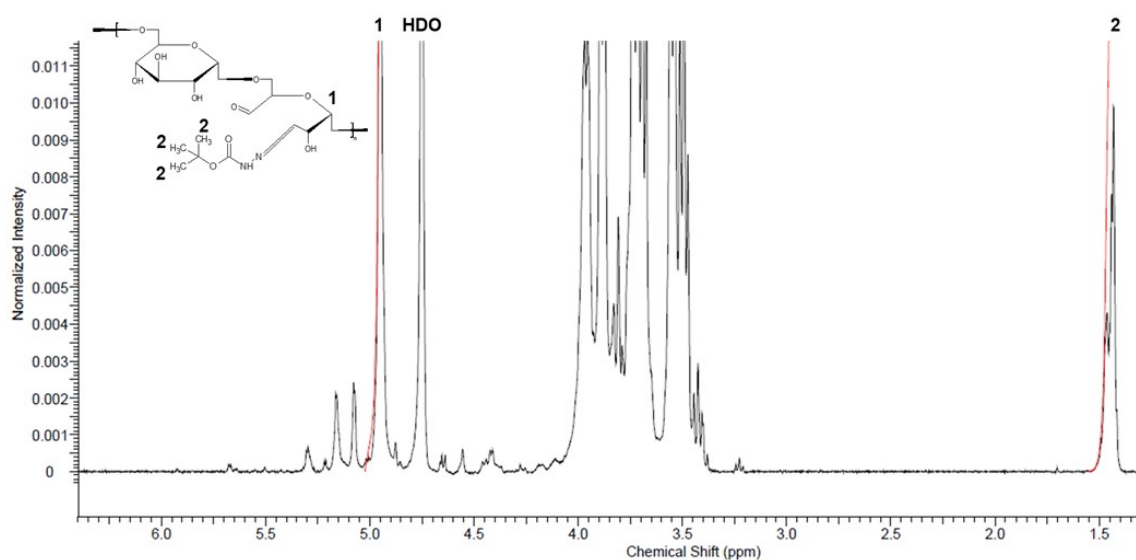
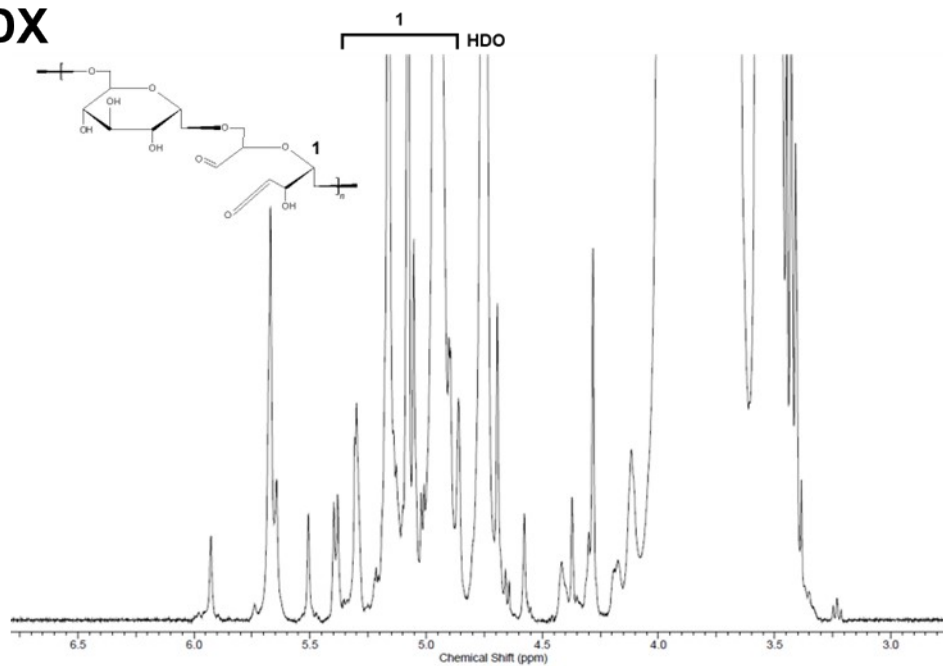
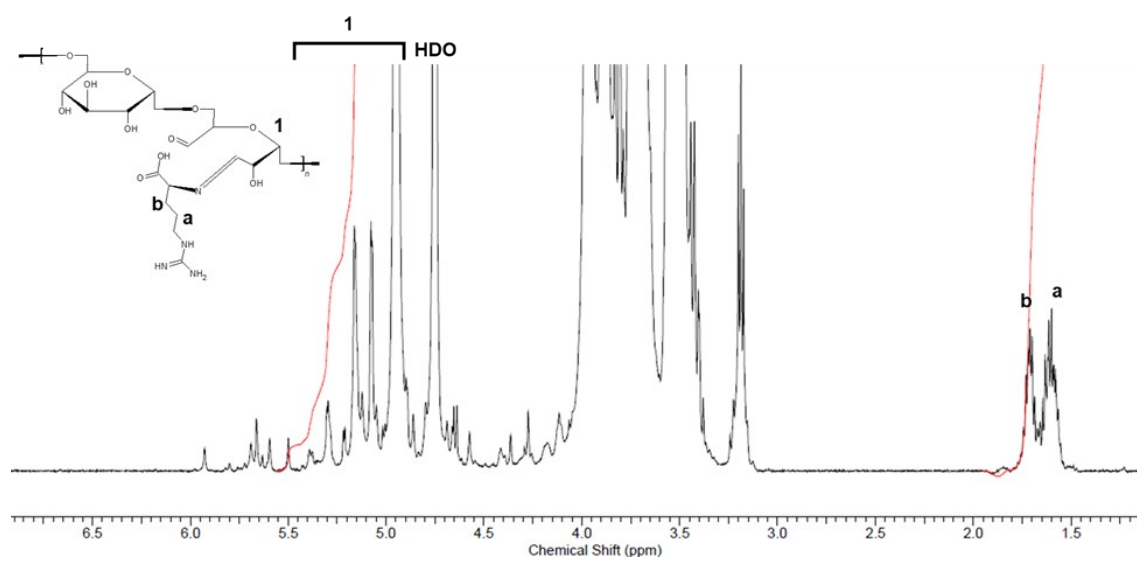


**Figure S1. The chemical structure and corresponding <sup>1</sup>H-NMR spectrum of dextran (DX) aldehyde modified with tert-butyl carbamate. The aldehyde degree of modification is estimated with <sup>1</sup>H NMR spectroscopy (300 MHz, D<sub>2</sub>O, residual internal HDO  $\delta$  4.75 as reference) by comparing the ratio of the integral peaks of tert-butyl protons:  $\delta$  1.39 – 1.49 (9H, -(CH<sub>3</sub>)<sub>3</sub>) to pyranose unit of DX:  $\delta$  4.87 – 5.29 (1H, C1)**

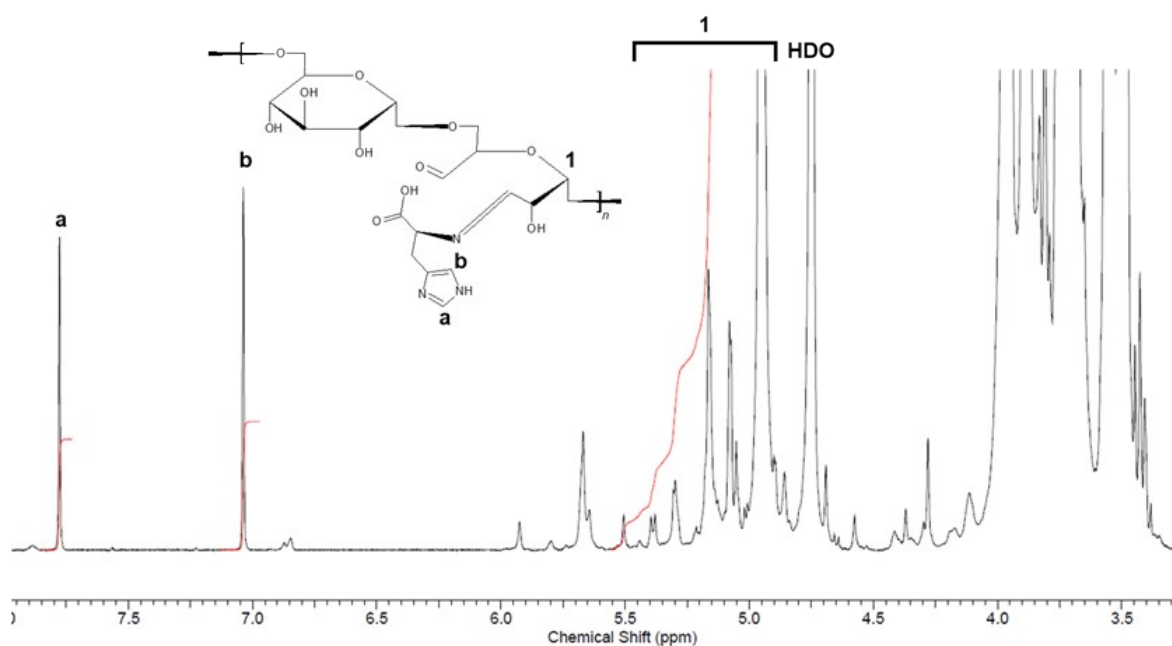
## A. DX



## B. ArgDX



## C. HisDX



## D. GlutDX

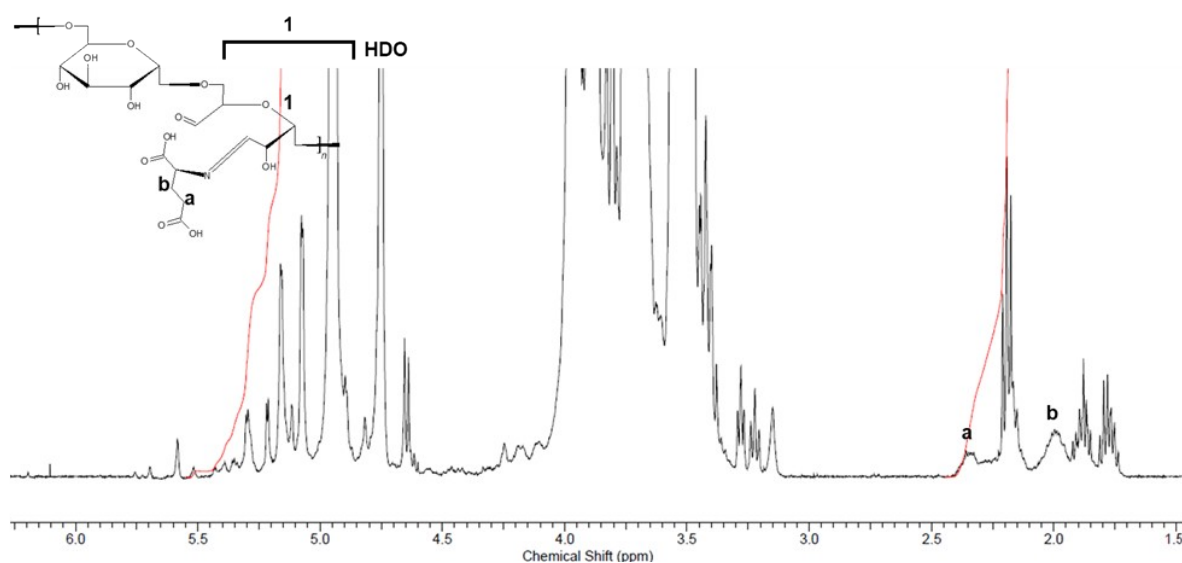


**Figure S2. The chemical structures and corresponding <sup>1</sup>H-NMR spectra of A) dextran (DX) aldehyde modified with B) L-arginine (ArgDX), C) L-histidine (HisDX) and D) L-glutamate (GlutDX).** Degree of modification of amino acids addition was estimated with <sup>1</sup>H NMR spectroscopy (300 MHz, D<sub>2</sub>O, residual internal HDO δ 4.75 as reference) by comparing the ratio of the integral peaks (δ) of H<sub>β</sub> and H<sub>γ</sub> of Glu: δ 2.25 (2H, -CH<sub>2</sub>) and 2.55 (2H, -CH<sub>2</sub>), H<sub>β</sub> and H<sub>γ</sub> of Arg: δ 1.5 (2H, -CH<sub>2</sub>) and 1.7 (2H, -CH<sub>2</sub>), and C-H ring H of His: δ 6.5 (1H, -CH-) and 8.5 (1H, -CH-) to pyranose unit of DX: δ 4.87 – 5.29 (1H, C1).

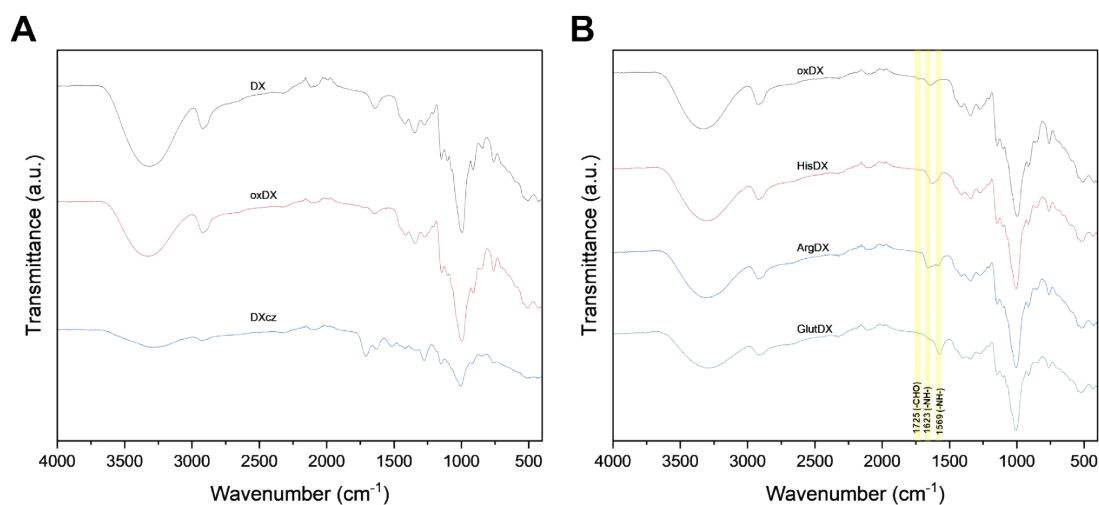


**Figure S3.** The FT-IR spectra of **A)** dextran (DX), DX aldehyde (oxDX) and DX carbazate (DXcz) and **B)** amino-acid modified oxDX, HisDX, ArgDX and GlutDX precursors.  $\nu = 1725 \text{ cm}^{-1}$  (C=O stretch),  $\nu = 1569 \text{ cm}^{-1}$ ,  $1623 \text{ cm}^{-1}$  (N-H bends of primary and secondary amines of amino acids modified on DX backbone).

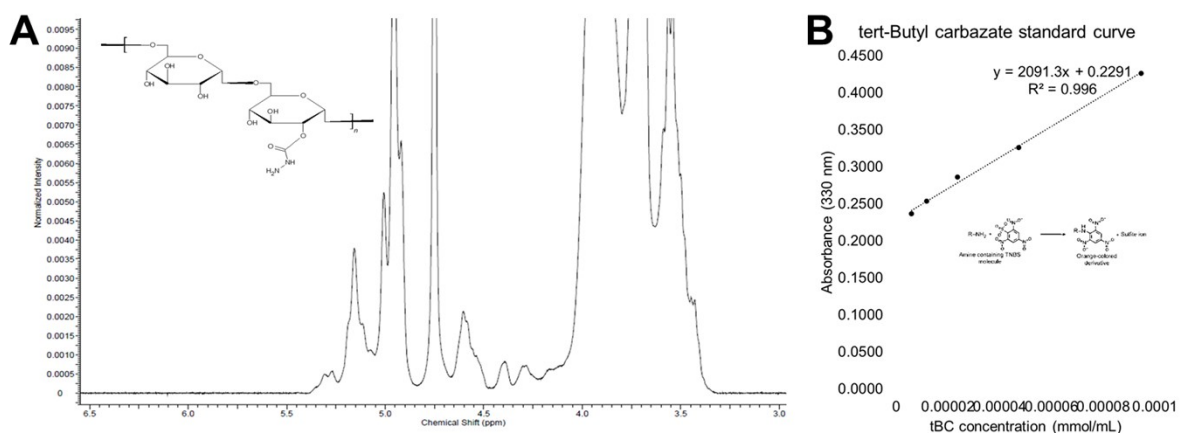


**Figure S4.** **A)** The chemical structure and corresponding  $^1\text{H-NMR}$  spectrum of DX carbazate. The degree of modification (DM) of carbazate on DX was determined from **B)** the standard curve of tert-butyl carbazate measured in TNBS assay.

**Table S1.** Summary of experimental degree of modification (DM) of precursors used in this study. oxDX: oxidized dextran, DXcz: dextran carbazate. ArgDX, HisDX and GlutDX: DX modified with L-arginine, L-histidine and L-glutamate respectively.

| <b>Precursors</b> | <b>Experimental DM%</b> |
|-------------------|-------------------------|
| oxDX              | 57.2                    |
| DXcz              | 40.6                    |
| ArgDX             | 4.8                     |
| HisDX             | 3.3                     |
| GlutDX            | 6.0                     |

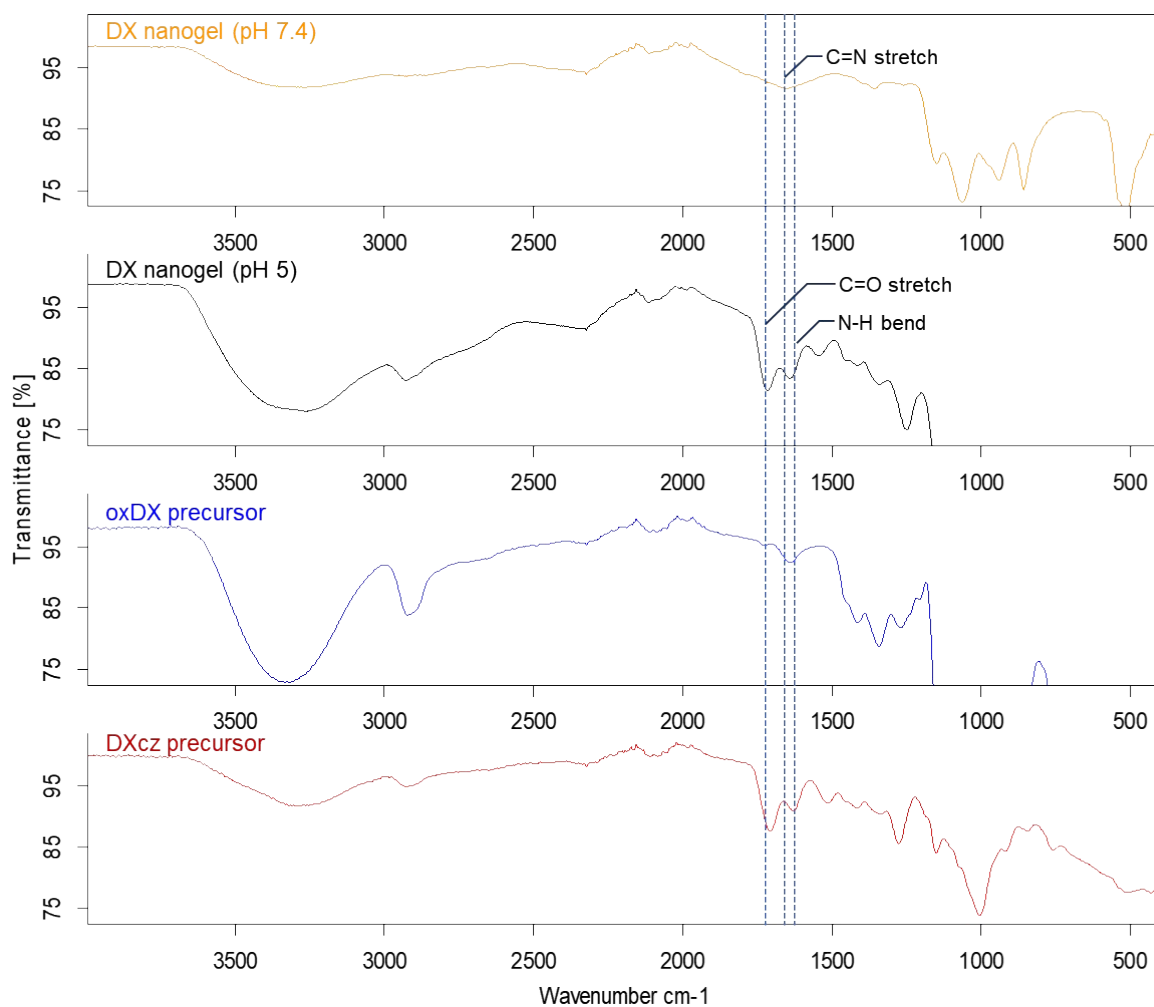


**Figure S5.** The FT-IR spectra of DX nanogel post-swelling in respective buffers of pH 5 and pH 7 and lyophilized. The spectra are compared to oxDX and DXcz precursors. For nanogel at pH 5, the disappearance of C=N stretch ( $1650 \text{ cm}^{-1}$ ) and reappearance of aldehyde C=O stretch ( $1725 \text{ cm}^{-1}$ ) and N-H bend ( $1625 \text{ cm}^{-1}$ ) peaks indicate the hydrolysis of acylhydrazone under acidic conditions.

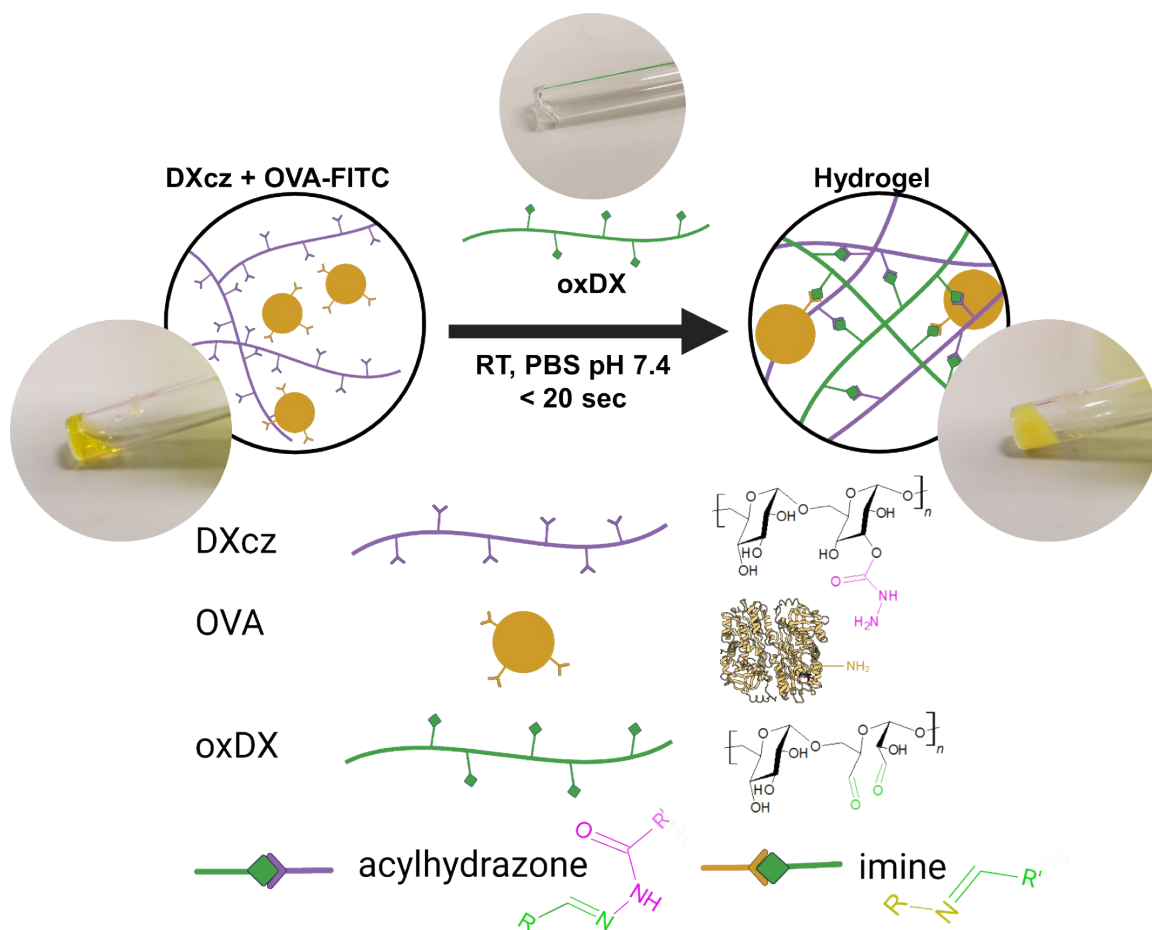


**Figure S6.** The reaction between the aldehyde groups on oxDX with the carbazate on DXcz and primary amine on OVA surface to form acylhydrazone and imine bonds respectively. The resulting hydrogel network was sensitive to acid-induced hydrolysis of the crosslinkers.

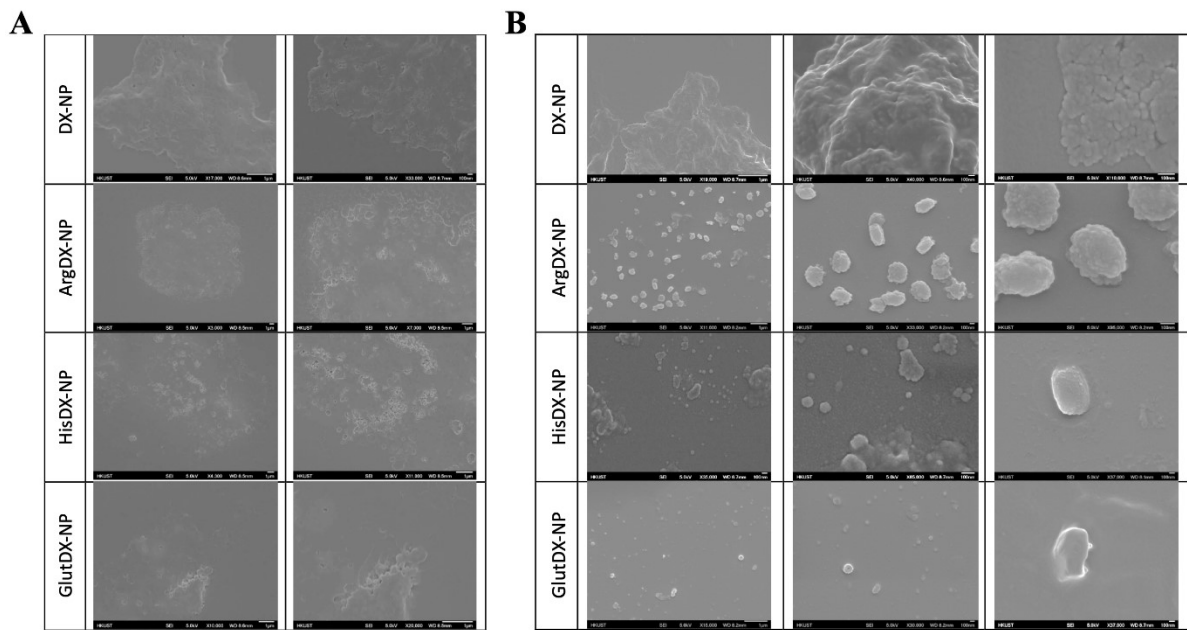


**Figure S7.** FESEM images of different empty DX nanoparticles (NP) in A) Acetone solvent and B) Methanol solvent. An acceleration voltage of 5.0 kV was utilized for all field emission scanning electron microscope (FESEM) images, and scale bars are provided at the bottom of each photo.



**Figure S8.** Macroscopic assessment of the safety of nanogels. Representative images of the injection sites on day 7 post-treatment. 150  $\mu$ L of nanogels, i.e. DX, ArgDX, GlutDX, HisDX were suspended in PBS. OVA were also prepared in alum and PBS (bolus), serving as controls. All injection contents were administered subcutaneously at the dorsal region. No treatment-associated local adverse effects were observed in the animals, regardless of the test groups. The skin area at the injection sites were examined. Granulomas associated with subcutaneous vaccines were present in nanogel treatment groups and alum. Similar findings on alum adjuvants have been reported in other studies. These effects were considered acceptable side effects and were associated with the translocation of vaccines to regional lymph nodes, driven by the resident innate immune cells. Furthermore, the mice remained active and showed no prominent weight loss and tissue waste, indicating minimal systemic side effects post-treatment.

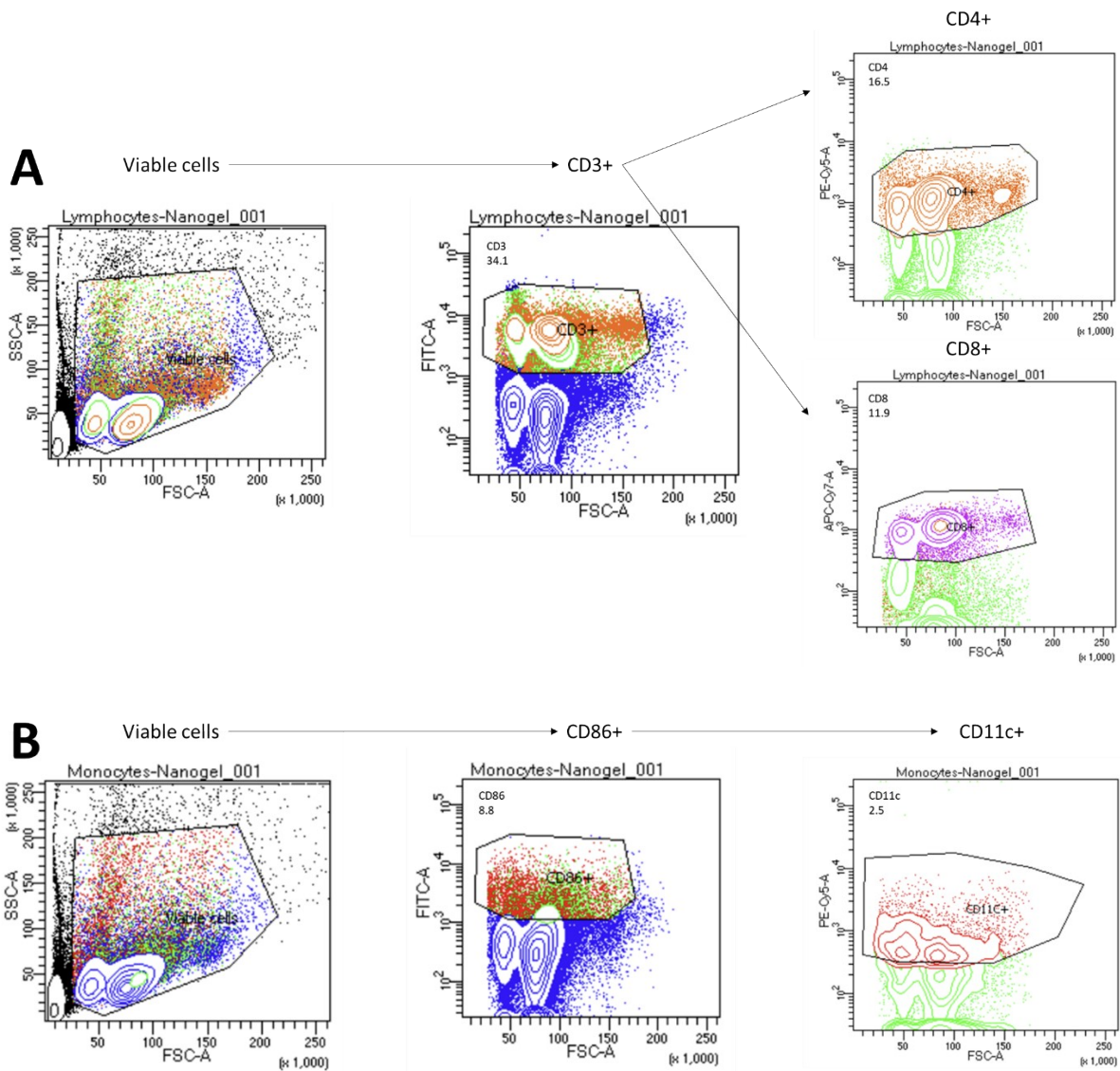


**Figure S9.** Representative flow cytometry images obtained from ILN samples of C57BL/6 mice on day 7 post-nanogel treatment. Gating strategies are shown for A) CD3+, CD4+ and CD8+ T-cell subpopulations and B) CD11c+ cells with activation marker CD86+. %total for each subset is labelled in the graphs.

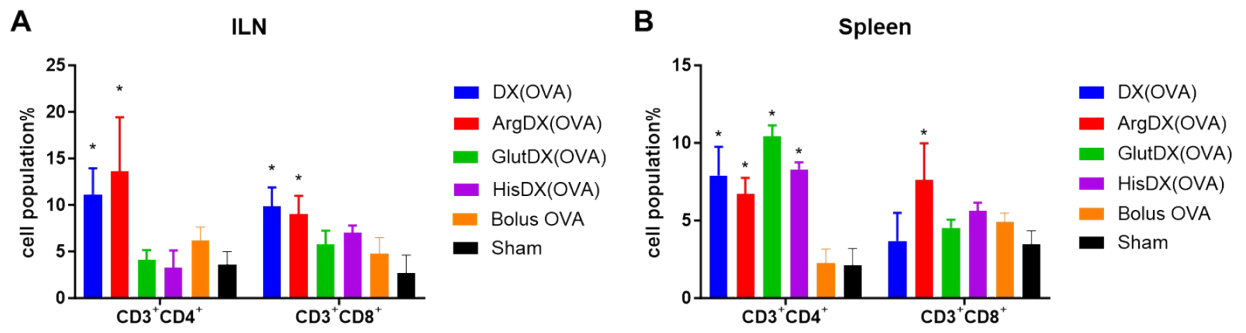


**Figure S10.** Anti-OVA cellular responses triggered by OVA-laden nanogels in comparison to bolus OVA and sham group (unimmunized mice). T-cell subsets, CD3<sup>+</sup>CD4<sup>+</sup> and CD3<sup>+</sup>CD8<sup>+</sup> in A) spleen and B) ILN were evaluated on day 7 post-subcutaneous injections. (N ≥ 4, where \* is in comparison to sham group, p < 0.05).